

Nonlinear optical waveguides fabricated in Mg-doped LiNbO₃ by swift heavy ion irradiation: anomalous photorefractive damage behavior

M. Jubera · A. Garcia-Cabañes · M. Carrascosa · J. Olivares

Received: 25 March 2013 / Accepted: 7 November 2013 / Published online: 30 November 2013
© Springer-Verlag Berlin Heidelberg 2013

Abstract Using swift heavy fluorine ion irradiation, we have successfully fabricated optical waveguides in Mg-doped LiNbO₃ substrates. A systematic characterization of these structures has been carried out including refractive index profiles, propagation losses, nonlinear coefficients, and, specially, photorefractive optical damage. Step-like refractive index profiles with $\Delta n_e \approx 0.1$ and $\Delta n_o \approx 0.2$, propagation losses lower than 0.5 dB/cm and high nonlinear optical coefficients similar to those of the substrate have been obtained. Unexpectedly, the photorefractive damage is only moderately reduced with regard to the one presented in congruent LiNbO₃ waveguides. Specifically, light intensity damage thresholds I_{th} are only a factor 2 higher at RT and a factor 4 at 90 °C with regard to undoped waveguides. At this latter temperature, a remarkably high $I_{th} = 30.000 \text{ W/cm}^2$ is reached. A final discussion on the observed anomalous optical damage behavior induced by swift heavy ion irradiation is also included.

1 Introduction

Recently, a novel method to fabricate optical waveguides in LiNbO₃ (and other crystals) has been proposed and

tested [1–4]. It uses medium-mass (also called *heavy*) ions at relatively high energies in the range 5–50 MeV, i.e. *swift heavy ion irradiation* (SHI), in order to have the maximum electronic stopping power placed a few microns inside the substrate. It requires much shorter irradiation fluences (10^{13} – 10^{15} cm^{-2}) than conventional ion implantation [5, 6] that uses low energy light ions. In this method, ions, energies, and fluences are selected so that electronic damage generates a buried amorphous layer a few microns beneath the surface [2]. At variance with conventional ion implantation, amorphization rely only on the electronic energy deposition (electronic stopping power) and not on elastic nuclear collisions (nuclear stopping power). In addition, the amorphous layer that acts as an optical barrier can be designed wide enough to minimize tunneling propagation losses [7] and is free of foreigner ions that stop deeper in the sample. The optical waveguides fabricated by this method present very good linear and nonlinear optical properties such as: step-like refractive index change for extraordinary ($\Delta n_e \approx 0.1$) and ordinary ($\Delta n_o \approx 0.2$) polarizations, high nonlinear optical coefficients reaching values only a 30 % lower than those of the substrate [1], and low propagation losses (under 0.5 dB/cm) when using suitable post-fabrication annealing treatments [7]. Moreover, it has also been demonstrated that periodically poled waveguides can be obtained [8]. Most works present results on planar waveguides, and channel waveguides have also been fabricated although the reported propagation losses are larger (8 dB/cm) [9].

For efficient nonlinear optical frequency conversion and other high power photonic applications, it is also necessary to reduce the photorefractive optical damage (POD) [10, 11]. This phenomenon consists in a light-induced refractive index change Δn that produces beam degradation during propagation and light intensity limitation effects [12, 13].

M. Jubera (✉) · A. Garcia-Cabañes · M. Carrascosa
Dpto. de Física de Materiales, Universidad Autónoma de Madrid, 28049 Madrid, Spain
e-mail: mariano.jubera@uam.es

J. Olivares
CMAM, Universidad Autónoma de Madrid, 28049 Madrid, Spain

J. Olivares
Instituto de Óptica, CSIC, Serrano 121, 28016 Madrid, Spain

Our very recent measurements [14, 15] in congruent SHI LiNbO₃ waveguides show moderate POD levels, similar to that of proton exchanged waveguides [13], but already requiring light intensities below 100 W/cm² to avoid optical damage at room temperature. Then, for high-power applications, such as second harmonic generation, a further inhibition of POD would be very convenient. To this end, a few methods have been proposed [12, 16, 17]. Substrate doping with damage-resistant impurities, particularly Mg doping, is probably the most simple and flexible approach and it is often used [18–20]. Moreover, Mg doping reduces the coercive field of LiNbO₃ facilitating domain inversion and periodic poling for quasi-phase matching applications [21]. However, SHI LiNbO₃ waveguides have been only prepared in undoped congruent LiNbO₃ so far. In fact, there are some recent works reporting implantation of Mg:LiNbO₃ with oxygen ions but with energies in the range 1–5 MeV [22, 23] still too low to generate a dominant electronic amorphization. In fact, a different kind of waveguides with lower refractive index jumps and thinner optical barriers are obtained. Moreover, these works do not present any optical damage characterization.

In this work, we have fabricated for the first time to our knowledge optical waveguides in Mg-doped LiNbO₃ substrates by irradiation with swift heavy fluorine ions. Then, an in-depth characterization of these waveguides is addressed including refractive index profiles, propagation losses, and nonlinear optical susceptibilities. Particular attention has been paid to characterize POD. Both polarizations TE and TM have been considered, and the effect of raising temperature as a procedure for a further inhibition of the POD has been investigated. The results are compared with previous works on SHI waveguides using undoped substrates. Finally, a detailed discussion of the anomalous behavior found for the POD results is also presented.

2 Experimental techniques: fabrication and characterization

2.1 Fabrication process: swift heavy ion irradiation

The starting substrates were commercially available Z-cut 5 % Mg-doped LiNbO₃ plates purchased from Photox Inc. The waveguides have been fabricated by SHI on the Z+ surface of the LiNbO₃ substrates in the Tandetron accelerator of the CMAM of the Universidad Autónoma de Madrid [24]. Fluorine ions F⁴⁺ with energies in the range 20–30 MeV and fluences in the range $3\text{--}4 \times 10^{14}$ ions/cm² have been used. These irradiation parameters allow obtaining buried electronic damage-induced amorphous barriers wide enough to avoid tunneling propagation losses

[7]. Ion beam currents were kept in the range 50–100 nA to prevent excessive charging and heating. Since the available ion beam section was limited to 8×8 mm², normal or oblique ion incidence has been applied depending on the required waveguide length. The ion energy has been slightly modified to keep a similar thickness for all waveguides. The irradiation duration was about 30–45 min. In Table 1, a relation of the various waveguides used in this work is presented. Some waveguides have been fabricated in pure congruent LiNbO₃ substrates with the same irradiation parameters for comparison purposes.

After irradiation, 1-h thermal annealing in air at $T \geq 300$ °C has been carried out to remove color centers and defects produced by irradiation. With these treatments, propagation losses can be markedly reduced.

2.2 Determination of the refractive index profile and the propagation losses

The refractive index profile of the waveguides have been characterized by measuring the refractive index TE (ordinary refractive index n_o) and TM (extraordinary refractive index n_e) profiles using the prism-coupling *m*-line method with $\lambda = 632.8$ nm. The technique requires determining the effective indexes of the propagating modes by measuring the coupling angles to the waveguide through an isosceles rutile prism. With this information, the profile can be accurately reconstructed through a reverse IWKB algorithm since the fabricated guides support a high enough number of modes (4–7).

Propagation losses (PL) were determined from the intensity profile of the scattered light during propagation (at $\lambda = 632.8$ nm) recorded by a CCD camera [25].

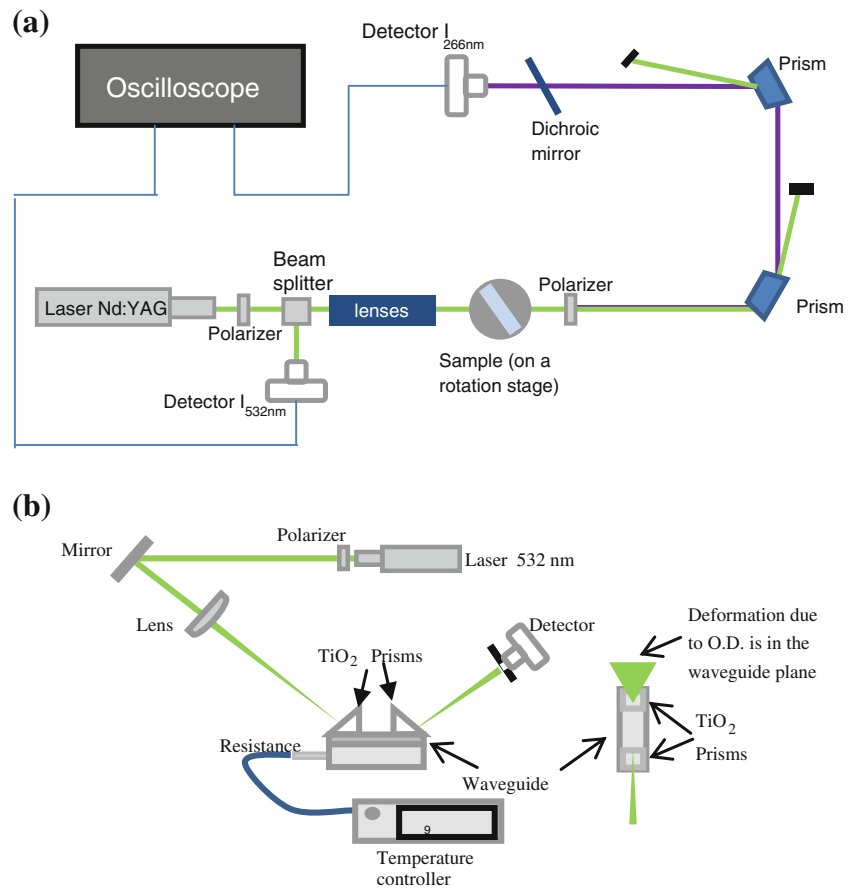
2.3 Measurement of the nonlinear coefficient d_{33}

The second-order nonlinear optical response has been evaluated by using the method described in detail in Ref. [26] for transmission geometry. The experimental setup is shown in Fig. 1a. As fundamental beam, we use the 532 nm output of a frequency-doubled Nd:YAG pulsed laser. The laser beam propagates through the LiNbO₃ plate with a peak intensity of 10⁸ W/cm². This generates along the beam path a second harmonic beam at 266 nm wavelength that lies well inside the ultraviolet (UV) absorption edge of LiNbO₃ (320 nm) so that only the signal coming from a very thin surface layer (around 50 nm thickness) of the waveguide can be probed. Two Pellin Broca dispersive prisms are used to separate the fundamental and UV beam. After a dichroic mirror which reflects the remaining green light, the UV light intensity is collected by a photomultiplier connected to an oscilloscope. In order to obtain a relative value of d_{33} with regard to the substrate, the

Table 1 Fabrication parameters and characteristics of waveguides used in the present paper

Waveguide type	Substrate	Ion energy (MeV)	Ion fluence (ion/cm ²)	Irradiation angle	Waveguide thickness (μm)	Annealing treatment
A	Mg: LiNbO ₃	30	3 × 10 ¹⁴	70°	2	1 h 350 °C
B	LiNbO ₃	30	3 × 10 ¹⁴	70°	2	1 h 350 °C
C	Mg: LiNbO ₃	25	3 × 10 ¹⁴	45°	3.1	1 h 350 °C
D	LiNbO ₃	25	3 × 10 ¹⁴	45°	3.1	1 h 350 °C
E	Mg: LiNbO ₃	20	4 × 10 ¹⁴	0°	3	1 h 300 °C

Fig. 1 a Experimental setup for the determination of the nonlinear coefficients.
b Experimental setup (frontal and zenithal view) to measure IDT at different temperatures



measurement has been carried out for both the LiNbO₃ substrate and the SHI waveguide.

2.4 Photorefractive optical damage

Special attention has been paid to the study of POD, because its inhibition is the main motivation to fabricate waveguides in Mg-doped substrates.

To this end, we first determined at what light intensity optical damage effects appear. This intensity is often called light intensity damage threshold (IDT) [15, 27]. A standard single-beam method using in- and out-coupling rutile prism-

couplers, as described in [15], and schematically shown in Fig. 1b, was used to determine light intensity damage thresholds (IDT). The IDT is more specifically defined by the in-coupled intensity I_{in} at which the out-coupled intensity I_{out} is no longer proportional to I_{in} . Then, this magnitude determines the range of intensities at which one can safely work without beam degradation along propagation. While continuously illuminating the waveguide with light at $\lambda = 532$ nm, the output power passing through a diaphragm placed 20 cm behind the waveguide is monitored. The size of the diaphragm is chosen such that at low intensities (no optical damage), about 70 % of the total out-coupled power

is transmitted. This way, the dependence I_{out} versus I_{in} loses the linearity when the beam starts to distort.

In order to obtain more information about the light beam quality, particularly above the IDT, the two-dimensional intensity profile of the out-coupled beam has been captured by a light intensity profilometer. Note that the deformation of the beam is produced in the guide plane, perpendicularly to the direction of confinement. For experimental reasons, the guide is placed with such direction parallel to the optical table. Thus, in the image spot obtained with the profilometer, the beam is distorted vertically, whereas the horizontal axis corresponds to the direction of confinement, in which the beam is not deformed.

The determination of the light intensity inside the waveguide is a key point in both experimental techniques. In all we evaluated the light intensity inside the waveguide I_{in} just at the input point, i.e., next to the first coupling prism, using the procedures described in [28]. With this method, a 10–15 % error in the determination of light intensity is estimated.

3 Results

3.1 Refractive index profile and propagation losses

We measured the refractive index profiles for all waveguides obtaining similar step-like profiles. Figure 2 illustrates these results for waveguides A, B [see Table 1] fabricated with the same ion irradiation parameters in undoped and Mg-doped LiNbO_3 substrates. The horizontal lines indicate the extraordinary refractive index of the Mg-doped (green line) and congruent (red line) substrates, respectively. It can be seen that for each polarization, the index profiles in both type of substrates are surprisingly very similar within the experimental error. This occurs because, as it can be clearly appreciated in the inset of the figure, the extraordinary index of the Mg-doped surface layer significantly increases during irradiation ($\Delta n_{e,\text{surf}} = 0.009$) so that it reaches a value similar to that of the congruent substrate and SHI waveguide. In summary, we also found for Mg-doped SHI waveguides step-like shape for TE and TM polarizations with very high refractive index jumps of $\Delta n_e \approx 0.104$ and $\Delta n_o \approx 0.183$ (at $\lambda = 630$ nm). They are 1–2 orders of magnitude larger than those exhibited by PE and Ti in-diffusion and are also higher than those presented by typical light ion implantation LiNbO_3 guides [6, 29–31]. The behavior under irradiation of the surface extraordinary refractive index is remarkable, which approaches the value of congruent LiNbO_3 , is remarkable, and will be discussed in Sect. 4.

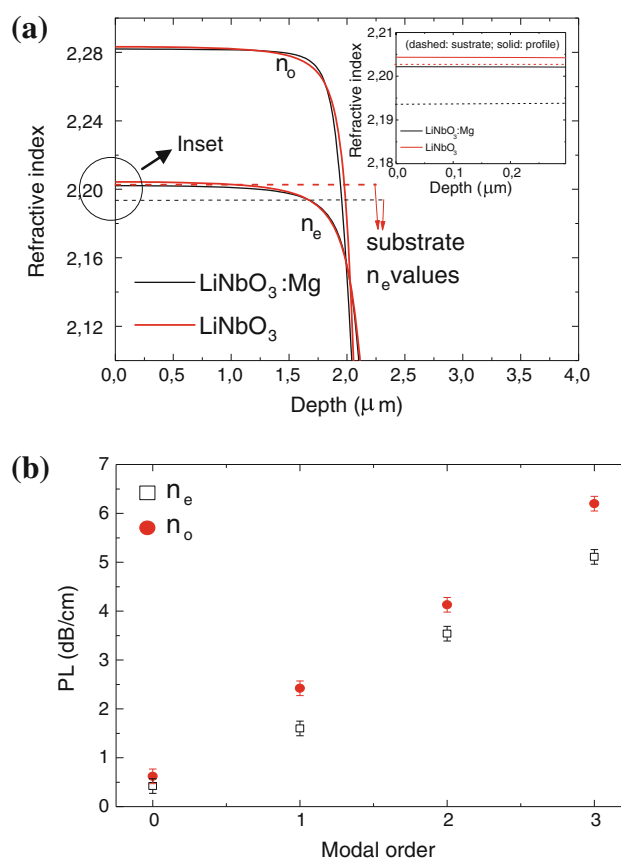


Fig. 2 **a** TE and TM refractive index profiles as a function of the depth h for undoped and Mg-doped waveguides. The *inset* shows a zoom of the surface refractive indexes of the waveguides. The substrate refractive index values are also plotted with *dashed lines* for comparison. **b** Measured propagation losses (PL) for a SHI type C waveguide and for the first four modes and TE and TM polarizations

In the early development of SHI waveguides, propagation losses (PL) range in the interval 1–10 dB/cm. Recently, by means of annealing treatments, propagation losses under 0.5 dB/cm have been obtained in waveguides fabricated on nominally pure congruent substrates [7]. Then, we have subjected the irradiated Mg-doped samples to the same annealing treatments (1 h at 350 °C). The results for the four first modes and TE and TM polarizations are shown in Fig. 2b using waveguide type C. The propagation losses for the fundamental mode are 0.4 and 0.6 dB/cm for TE and TM polarizations, respectively. These remarkably low values are similar to those obtained with undoped (congruent) waveguides [7].

For successive higher modes, increased propagation losses are observed. This can be understood taken into account that higher order modes are progressively less confined so that they are more affected by the higher concentration of scattering defects existing, most likely, at the boundary with the amorphous layer.

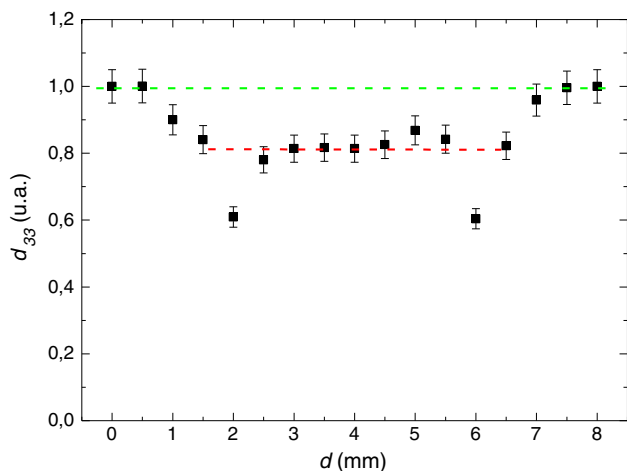


Fig. 3 Second-order nonlinear coefficient measured along a longitudinal axis of the sample for a type E waveguide

3.2 Nonlinear optical coefficients

In order to obtain an accurate determination of the relative value of d_{33} , we have irradiated only a central ($4 \times 4 \text{ mm}^2$) region of the Mg-doped substrate, $10 \times 10 \text{ mm}^2$ size, using normal incidence (guide type E). In this way, the d_{33} values corresponding to an irradiated and non-irradiated (virgin) substrate can be measured in the same sample. Figure 3 shows the results for the d_{33} profile along a longitudinal axis of the sample. In the irradiated region, d_{33} is approximately constant with a value 80 % of those of the extremes corresponding to the non-irradiated substrate.

Note that the obtained d_{33} profile clearly indicates the limits of the irradiated region and can be considered an additional tool to characterize the quality and homogeneity of the irradiation method. It is worthwhile remarking that the obtained relative values of d_{33} are even slightly larger than those reported for congruent undoped substrates at the same fluence about 70 % [1, 2].

3.3 Photorefractive optical damage

Photorefractive optical damage has been characterized in waveguides of type C, long enough to obtain accurate results. First, we determined the IDT by measuring the decoupled intensity versus the coupled intensity for both ordinary and extraordinary polarizations in the guides. The results are shown in Fig. 4. The dependence is linear up to a value of $\sim 50 \text{ W/cm}^2$ for extraordinary polarization and $\sim 100 \text{ W/cm}^2$ for ordinary polarization, i.e., these are the IDT values for TE and TM fundamental modes, respectively.

To characterize the beam distortion above the IDT, the output beam intensity profiles for different intensities and

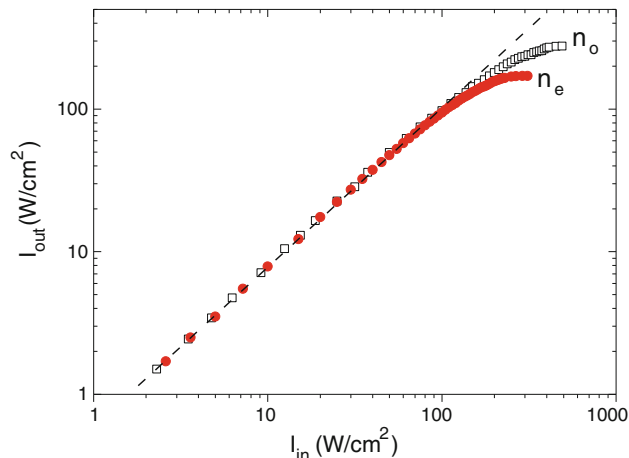


Fig. 4 Logarithmic plot of the output intensity I_{out} versus input intensity I_{in} inside the waveguide for TE (squares) and TM (circles) propagating fundamental modes. The propagation length is 7 mm

for both polarizations have been recorded by a beam profilometer. These profiles for five increasing input light intensities are shown in Fig. 5 for TM (a) and TE (b) modes. The beam propagation length is 7 mm as in Fig. 4. It can be clearly seen that above the IDT a self-defocusing effect accompanied by distortion of the beam profile appears that becomes more and more important as I increases. This behavior clearly explains the loss of the linearity in Fig. 4: due to beam deformation, the power fraction passing the diaphragm of the corresponding setup decreases progressively for both polarizations.

In order to compare the POD in Mg-doped and undoped congruent waveguides, we have also measured the IDT in waveguide D fabricated in an undoped substrate with the same irradiation parameters (see Table 1). The obtained curves for the fundamental TE mode (n_o) are plotted in Fig. 6.

It can be seen that the IDT has increased a factor 2 in the Mg-doped samples, although this factor is much lower than the ones reported in the literature for congruent and Mg-doped crystals and PE waveguides that range between 10 and 1,000 [20, 32, 33].

3.4 Temperature optical damage inhibition

A method to obtain a further decrease in optical damage successfully used in bulk congruent crystals and other type of LiNbO_3 waveguides is to heat the sample [15, 16, 18].

Then, we determined the IDT at a temperature of $90 \text{ }^\circ\text{C}$, for the TE fundamental mode in the same congruent and Mg-doped samples of Fig. 6. The results are shown in Fig. 7a. By increasing the temperature to $90 \text{ }^\circ\text{C}$, intensities as high as 30 kW/cm^2 can be safely used in the Mg-doped LiNbO_3 waveguides without optical damage effects. Moreover, the IDT value is appreciably larger than in the

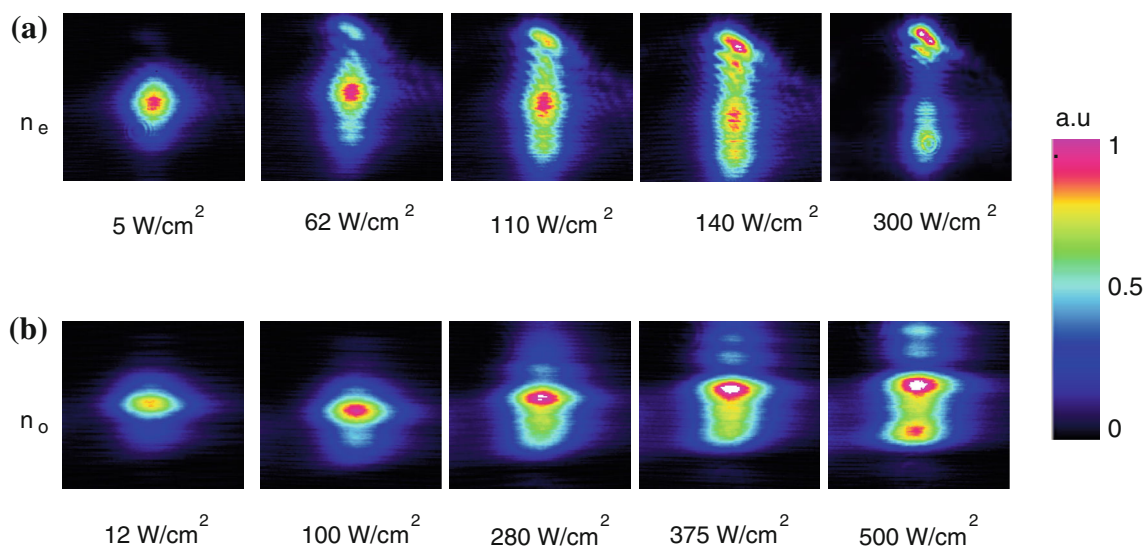


Fig. 5 Output beam intensity profiles at increasing intensities for **a** TM and **b** TE propagating fundamental modes

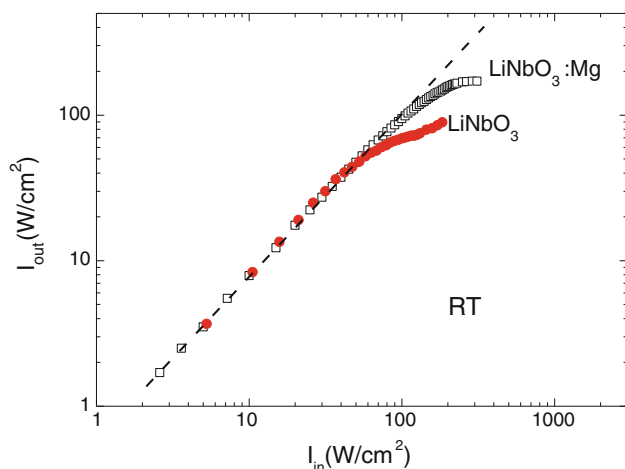


Fig. 6 Logarithmic plot of the output fundamental TE mode intensity I_{out} versus the input intensity I_{in} inside the waveguide for Mg-doped (squares) and undoped congruent (circles) substrates. The propagation length is 7 mm

congruent substrate (a factor 4). The evolution of the beam profile with temperature at a constant input intensity $I = 1,050 \text{ W/cm}^2$, well above the IDT at room temperature, for the Mg-doped waveguide is presented in Fig. 7b. It can be seen that a temperature of $55 \text{ }^\circ\text{C}$ is high enough to eliminate optical damage for this intensity value, whereas in a congruent substrate, it is necessary to go up to $75 \text{ }^\circ\text{C}$ [15]. Therefore, temperature results also show an appreciable reduction of POD in Mg-doped SHI waveguides.

4 Discussion

SHI waveguides can be fabricated on Mg-doped substrates with very similar refractive index profile to those obtained

in congruent samples. Moreover, the annealing process proposed in Ref. [7] to reduce propagation losses is also successful in this case. This confirms its ability to improve the quality of the SHI waveguides leading to PL values fully competitive.

Regarding the nonlinear properties, the measured nonlinear optical coefficient d_{33} is also comparable or even better to that reported for waveguides fabricated on congruent substrates [1, 2]. In turn, intensity damage thresholds increase a factor 2 at room temperature and up to a factor 4 as T increases until $90 \text{ }^\circ\text{C}$. However, the moderate reduction of optical damage compared with congruent waveguides is much lower than expected, deserving a particular analysis.

4.1 On the anomalous photorefractive damage behavior

Since the low effect of Mg doping on optical damage was unexpected, we have repeated the IDT measurements in several type C samples for confirmation. Similar results have been obtained in all experiments. Moreover, since recent experiments with swift He-implanted LiNbO_3 guides [34] show an influence of the irradiation direction ($+Z$ versus $-Z$) in some material properties (electrical conductivity and refractive index), we have also fabricated SHI waveguides irradiating the $-Z$ face and determined the IDT. However, no difference with previous $+Z$ irradiated samples has been found. In addition, to discard any uncontrolled problem with the particular Mg-doped LiNbO_3 wafer from which the substrates have been cut, we have measured the absorption spectrum, confirming that the absorption edge and OH IR band peak positions correspond to 5 % Mg doping, i.e., the correct doping for

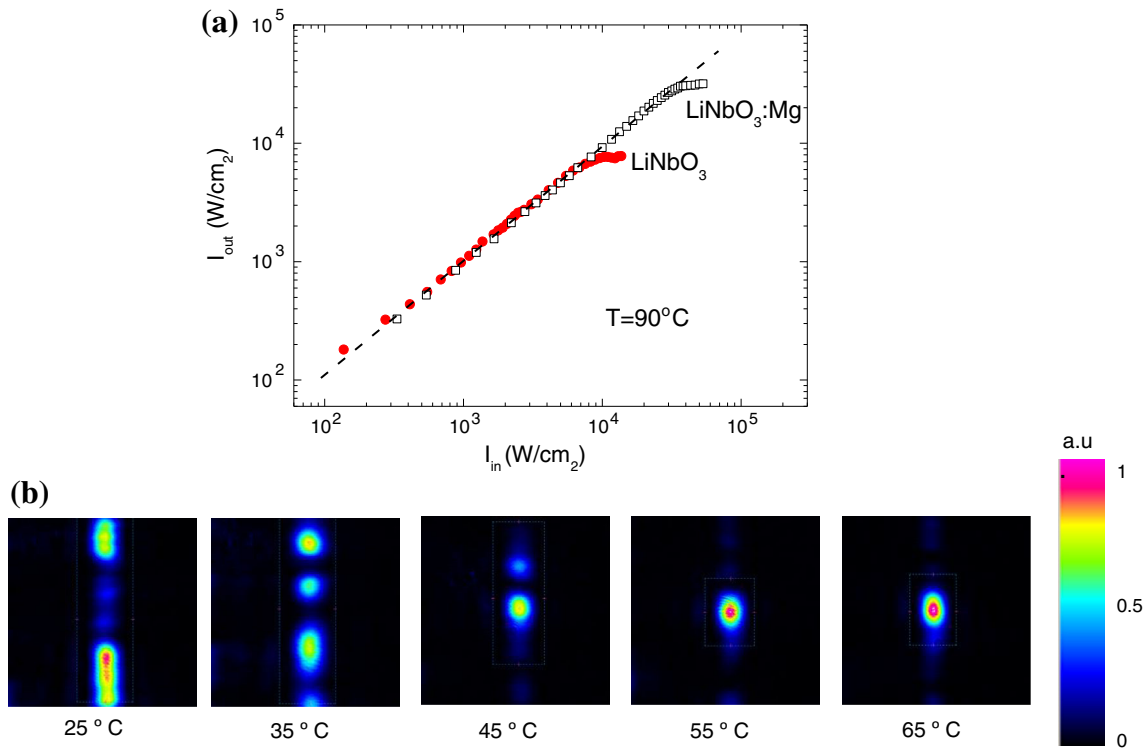


Fig. 7 **a** I_{out} versus I_{in} for the TE fundamental mode propagating in the Mg-doped (circles) and undoped congruent (squares) waveguides kept at 90 °C. **b** Output beam profile at increasing temperatures for a Mg-doped SHI waveguide at a light intensity of 1,050 W/cm²

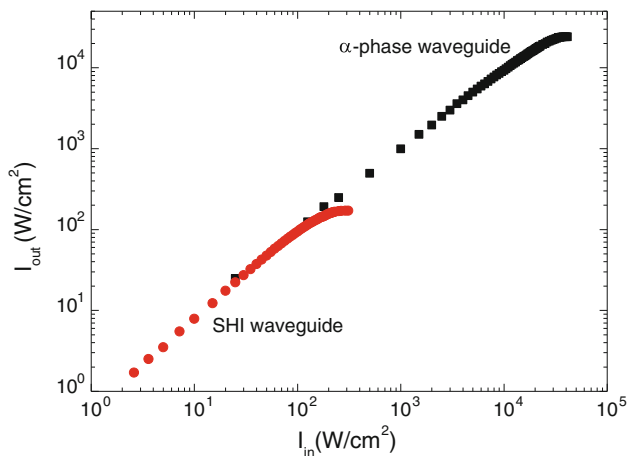


Fig. 8 I_{out} versus I_{in} for the fundamental extraordinary mode for a SHI (red circles) and α -phase PE (black circles) waveguide. The two waveguides were fabricated from the same LiNbO₃ wafer doped with Mg 5 %

optical damage inhibition. Finally, we have fabricated in a substrate from the same Mg-doped wafer a conventional α -phase PE waveguide and characterize its optical damage using the same techniques than in SHI waveguides. The result is shown in Fig. 8 where the curve for the SHI Mg-doped waveguide is also plotted for comparison. As reported in previous works [35] and at difference with the SHI waveguide, the α -phase PE Mg:LiNbO₃ guide presents

an IDT of about 10 kW/cm², i.e., two orders of magnitude higher than the IDT values reported for the corresponding undoped PE guides. From all these data, we can definitely confirm the only moderate reduction of POD in the case of SHI Mg-doped LiNbO₃ waveguides, at difference with other waveguide types (as α -phase PE). This anomalous behavior is very likely due to the fabrication method. In fact, a similar result has been reported in the literature for a more conventional Mg-doped LiNbO₃ waveguide obtained by low energy ion implantation [36].

A further step is to wonder about the origin of this lower reduction of optical damage. Some hints can be provided here. The accepted mechanism for optical damage inhibition is the elimination of Nb in Li-site defects, responsible for the photorefractive effect at high light intensities [37–40]. Then, the simplest explanation is that SHI generates this kind of defect recovering to some degree the photorefractive response. In fact, it is well known that local compositional as well as structural changes can be induced by irradiation, particularly, in insulating materials [3, 34, 41, 42]. This may occur by nuclear collisions as well as electronic processes during the irradiation. Possible mechanisms include atomic displacements, defect formation, and radiation-enhanced diffusion. In fact, the significant modification of the surface extraordinary refractive index during irradiation (see Sect. 3.1), approaching the

value of the congruent crystal, also points to the same mentioned mechanisms. Note that it is well known that the extraordinary refractive index of LiNbO₃ substantially increases as the Li/Nb ratio decreases approaching the congruent composition [43, 44] and that increase implies an enhancement on the number of Nb anti-sites. Anyhow, further work on this subject is necessary to fully characterize and explain these ion irradiation effects.

5 Conclusions

Swift heavy fluorine ion irradiation waveguides have been successfully fabricated in Mg-doped LiNbO₃ substrates. These waveguides keep the good properties already found for undoped guides: step-like refractive index profiles with $\Delta n_e \approx 0.1$ and $\Delta n_o \approx 0.2$, low propagation losses around 0.5 dB and high nonlinear optical coefficients similar to those of LiNbO₃ crystals. However, photorefractive damage shows an anomalous behavior with a much less reduction than in other types of LiNbO₃ waveguides. This last result, together with the observed significant enhancement of the surface extraordinary index after irradiation, points to defect composition changes produced in Mg-doped substrates by SHI not investigated so far.

Acknowledgments This work was supported by projects MAT2008-06794-C03 and MAT2011-28379-C03-01. A FPI fellowship is acknowledged by Mariano Jubera. We acknowledge the support of the technical team of the CMAM for the ion beam irradiations.

References

- J. Olivares, G. García, A. García-Navarro, F. Agulló-López, O. Caballero, *Appl. Phys. Lett.* **86**, 183501 (2005)
- J. Olivares, A. García-Navarro, G. García, F. Agullo-Lopez, F. Agullo-Rueda, A. García-Cabañes, M. Carrascosa, *J. Appl. Phys.* **101**, 33512 (2007)
- J. Manzano-Santamaría, J. Olivares, A. Rivera, F. Agulló-López, *N.I.M. Phys. Res. B* **272**, 271 (2012)
- A. García-Navarro, J. Olivares, G. García, F. Agulló-López, S. García-Blanco, C. Merchant, J.S. Aitchison, *N.I.M. Phys. Res. B* **249**, 177 (2006)
- F. Chen, X. Wang, K. Wang, *Opt. Mater.* **29**, 1523 (2007)
- P.D. Townsend, P.J. Chandler, L. Zhang, in *Optical effect of ion implantation* (Cambridge University Press, Cambridge, 1994)
- M. Jubera, J. Villarroel, A. García-Cabañes, M. Carrascosa, J. Olivares, F. Agulló-López, A. Méndez, J.B. Ramiro *Appl. Phys. B* **107**, 157 (2012)
- O. Caballero-Calero, A. García-Cabañes, M. Carrascosa, F. Agulló-López, J. Villarroel, M. Crespillo, J. Olivares, *Appl. Phys. B* **95**, 435 (2009)
- A. Majkic, M. Koechlin, G. Poberaj, P. Günter, *Opt. Express* **16**, 8769 (2008)
- L. Arizmendi, *Phys. Status Solidi* **201**, 253 (2004)
- D. Kip, M. Wesner, Photorefractive waveguides. in *Photorefractive Materials and their Applications I: Fundamental Phenomena*, ed. by P. Günter, J.P. Huignard (Springer, Berlin, 2006)
- T. Volk, M. Wolecke, N. Rubinina, Optical damage resistance in lithium niobate. in *Photorefractive Materials and Their Applications II* (Springer, Berlin, 2007)
- J. Villarroel, J. Carnicero, F. Luedtke, M. Carrascosa, A. García-Cabañes, J.M. Cabrera, *Opt. Express* **20**, 20852 (2010)
- J. Villarroel, M. Carrascosa, A. García-Cabañes, O. Caballero-Calero, M. Crespillo, J. Olivares, *Appl. Phys. B* **95**, 429 (2009)
- M. Jubera, A. García-Cabañes, M. Carrascosa, J. Olivares, F. Luedtke, *J. Opt. Soc. Am. B* **29**, 3000 (2012)
- J. Rams, A. Alcazar-de-Velasco, M. Carrascosa, J.M. Cabrera, F. Agulló-López, *Opt. Commun.* **178**, 211 (2000)
- M. Kösters, B. Sturman, P. Werheit, D. Haertle, K. Buse, *Nat. Photonics* **3**, 510 (2009)
- A. Ikeda, T. Oi, K. Nakayama, Y. Otsuka, Y. Fujii, Temperature and electric field. *Jpn. J. Appl. Phys.* **44**, 1407 (2005)
- W.M. Young, R.S. Feigelson, M.M. Fejer, M.J.F. Digonnet, H.J. Shaw, *Opt. Lett.* **16**, 995 (1991)
- S. Steinberg, R. Goring, T. Henning, A. Rasch, *Opt. Lett.* **20**, 683 (1995)
- Y. Chen, W. Yan, J. Guo, S. Chen, G. Zhan, *Appl. Phys. Lett.* **87**, 212904 (2005)
- L. Wang, B. Xiang, *Nucl. Instrum. Methods Phys. Res. B* **272**, 121 (2012)
- H.P. Liu, F. Lu, X.Z. Liu, R.F. Zhang, Q. Song, X.L. Wang, X.J. Ma, T.L. Yang, Y.B. Lu, Y.H. Li, *J. Phys. D Appl. Phys.* **41**, 065302 (2008)
- <http://www.cmam.uam.es>. UAM-CMAM
- Y. Okamura, S. Yoshinaka, S. Yamamoto, *Appl. Opt.* **22**, 3892 (1983)
- J. Rams, J.M. Cabrera, *J. Mod. Opt.* **47**, 1659 (2000)
- O. Caballero-Calero, A. García-Cabañes, J.M. Cabrera, M. Carrascosa, A. Alcázar, *J. Appl. Phys.* **100**, 093103 (2006)
- O. Caballero-Calero, J. Carnicero, A. Alcazar, G. de la Paliza, A. García-Cabañes, M. Carrascosa, J.M. Cabrera, *J. Appl. Phys.* **102**, 074509 (2007)
- M. Minakata, S. Saito, M. Shibata, S. Miyazawa, *J. Appl. Phys.* **49**, 467 (1978)
- D. Kip, *Appl. Phys. B* **67**, 131 (1998)
- A. Alcazar, J. Rams, J.M. Cabrera, F. Agulló-López, *J. Appl. Phys.* **82**, 15 (1997)
- Y. Furukawa, K. Kitamura, S. Takekawa, A. Miyamoto, M. Terao, *Appl. Phys. Lett.* **77**, 2494 (2000)
- D. Bryan, R. Gerson, H. Tomaschke, *Appl. Phys. Lett.* **44**, 847 (1984)
- L. Jentjens, N.L. Raeth, K. Peithmann, K. Maier, *J. Appl. Phys.* **109**, 124104 (2011)
- F. Luedtke, J. Villarroel, A. García-Cabañes, K. Buse, M. Carrascosa, *Opt. Express* **17**, 658 (2009)
- E. Glavas, J.M. Cabrera, P.D. Townsend, *J. Phys. D Appl. Phys.* **22**, 611 (1989)
- M. Carrascosa, J. Villarroel, J. Carnicero, A. García-Cabañes, J.M. Cabrera, *Opt. Exp.* **16**, 115 (2008)
- K. Buse, *Appl. Phys. B* **64**, 391–407 (1997)
- J. Carnicero, O. Caballero, M. Carrascosa, J.M. Cabrera, *Appl. Phys. B* **79**, 351 (2004)
- E. Jermann, J. Otten, *J. Opt. Soc. Am. B* **10**, 2085 (1993)
- R. Vitova, T. Zamani-Meymian, M.R. Peithmann, *J. Phys. Cond. Matter* **21**, 495401 (2009)
- K. Peithmann, P.D. Eversheim, J. Goetze, M. Haaks, H. Hattermann, S. Haubrich, F. Hinterberger, L. Jentjens, W. Mader, N.L. Raeth, H. Schmid, M.R. Zamani-Meymian, K. Maier, *Appl. Phys. B* **105**, 113 (2011)
- U. Schlarb, K. Betzler, *Phys. Rev. B* **48**, 15613–15620 (1993)
- N. Sisodia, R. Trivedi, R.K. Choubey, P. Sen, P.K. Sen, S. Kar, K.S. Bartwal, *Appl. Phys. A* **84**, 291–295 (2006)